SMALL-SCALE ROUGHNESS EFFECTS ON THERMAL IR SPECTRA

L. K. Balick [a, *], I. Danilina [b], A. Gillespie [b], J. Jolin [c], A. Mushkin [d]

[a] Space and Remote Sensing Sciences, Los Alamos National Laboratory, Los Alamos, NM, USA – lbalick@lanl.gov
[b] Earth and Space Sciences, University of Washington, Seattle, WA, USA – (arg3, Danilina)@uw.edu
[c] Physical Chemistry and Applied Spectroscopy, Los Alamos National Laboratory, Los Alamos, NM, USA – jolin@lanl.gov
[d] Geological Survey of Israel, Jerusalem IS, Mushkin@gsi.gov.il

Commission VII Symposium

KEY WORDS: Hyper spectral, Multispectral, Thermal, Infrared, Surface, Radiometry, Measurement

ABSTRACT:

Thermal infrared (IR) spectra of materials are affected by subpixel surface roughness that increases interactions between surface facets, thereby shifting the spectra toward a blackbody. Roughness also creates directional effects due to differential solar heating and view geometry. Three types of ground-based experiments were conducted to quantify roughness effects at scales of about 10 cm or less. First, a radiosity model was implemented and validated for natural and artificial surfaces using an imaging spectrometer. Area and resolution create practical computational limits so most simulations were performed at a resolution near 1 cm over a 1 m area. Surfaces were specified using laser profilometer data but can be simulated. Second, a well-calibrated radiometer was used to measure radiance for emissivity retrievals of different sized gravels and at different solar and view geometries. Finally, a reflectance spectrometer measured spectra for soft rocks sanded to different roughnesses.

Measurements of soft rocks with single mineral features (alabaster, soapstone, and chlorite) sanded to different roughnesses show a decrease of spectral peak height with roughness when the roughness scale is significantly larger than the wavelength. Precise measurements of two types of gravel, in three size classes of gravels, with a non-imaging spectrometer show an apparent saturation of roughness effects and a probable increase of directional effects with roughness. The modelling results show that a simple radiosity model can broadly simulate the effects of roughness. The shape of the roughness elements has a significant impact. Imaging spectrometers permit observation of small-scale spatial variations, which are not observed at pixel scales of a meter or more. Spectra go to blackbody spectra in small cracks and crevices.

1. INTRODUCTION

1.1 Background and Objectives

The radiance observed by remote sensing platforms varies significantly with subpixel surface roughness. Subpixel surface roughness occurs at spatial scales at which facets of the surface interact with each other resulting in multiple reflection or absorption/emission of photons but are not resolved in an image. The concept is quite simple but the spatial limits are not abrupt and hard to quantify. They vary with wavelength at the lower limit and pixel size at the upper limit. At the small end of the scale, facets or characteristic dimensions are large enough—on the order of 100 times the wavelength—that non-linear scattering processes are unimportant. At the upper limit, the dimensions need to be small enough so that a pixel contains a representative sample of the geometric variation of the surface: perhaps a tenth of the pixel area. The key concept is that subpixel roughness effects occur between surface facets that are not resolved in a remotely sensed image pixel. The net effects include darkening pixels in the reflectance domain, brightening pixels in the emissive domain (increasing both temperature and emissivity), reducing the depth of spectral features, and producing directional variations of observed radiance. Surfaces composed of different materials (stones in a soil matrix, for instance) will undergo non-linear spectral mixing when facets of different materials interact with each other. At thermal infrared wavelengths, the effect is that emissivity spectra are moved closer to a blackbody spectrum in which extremely rough surfaces or cavities have an emissivity approaching 1.0 at all wavelengths. (The effects are broadly similar with surface roughness and volume scattering, such as occurs with vegetation or loosely packed particles, but volume scatting is more complex.) This paper presents studies of subpixel roughness effects across a variety of spatial scales in the long-wave infrared (LWIR, 8– 14 μm) spectral range.

Because pixels can be quite large, they can contain subpixel surface roughness effects across a range of spatial scales and phenomena. Typically, one spatial scale dominates observations or, at least, one spatial scale is of primary interest. Therefore, studies of roughness effects often concentrate on a single scale or phenomenon.

1.2 Objectives

This paper presents summaries of four studies of subpixel roughness effects that range from the upper limits to the lower limits of spatial scales relevant to remote sensing. First, at the finest scale, spectral measurements of rock surfaces roughened with different grits of sandpaper are examined and related to micro-profilometer measurements of the surfaces.

* Corresponding author

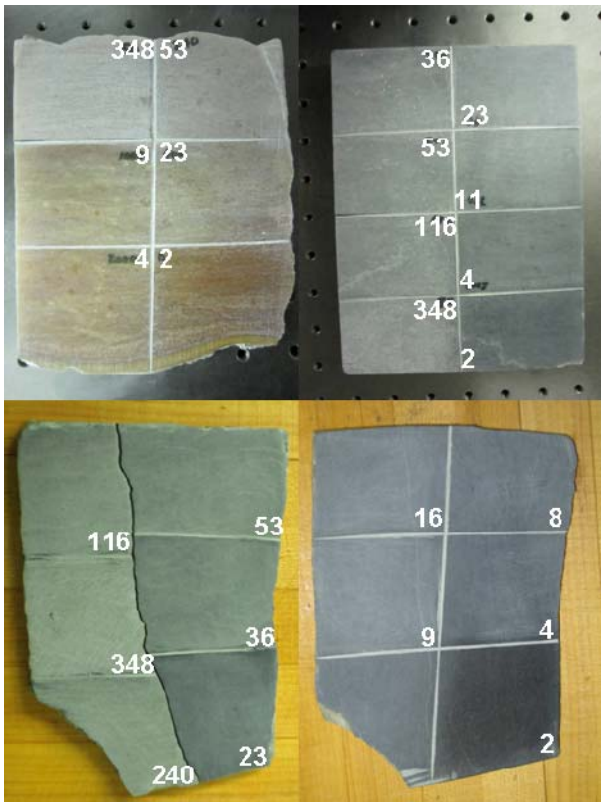

Figure 1. Flat rock surfaces sanded to U.S. grit sizes shown. Alabaster is at the upper left, soapstone at the upper right, and the two chlorite slabs are at the bottom.

Secondly, retrievals of emissivity of gravels of different sizes are made using data from a well-calibrated, highly stabilized FTIR spectrometer in the field, Balick & al., (2009). Third, a radiosity model of the impacts of roughness at centimetre scales was developed and verified. Simulations and data from special cases are presented. Finally, multi-directional satellite images are used to retrieve roughness information about the surface.

2. SURFACE ROUGHNESS STUDIES

2.1 Roughened Surfaces

Three types of fairly soft rocks were first smoothed and flattened, then hand-sanded with different grits, ranging from very smooth to very coarse and using diamond micromesh; about 2 μm to 350 μm average grit size. The rock types are commonly used in sculpture and are alabaster (gypsum, a sulfate), soapstone (talc, a phyllosilicate), and chlorite (another phyllosilicate closely related to soapstone). The rock surfaces and grit sizes are shown in Figure 1. Note that the different roughnesses vary in appearance in the visible wavelengths with the rougher surfaces appearing as a flat grey and becoming darker or more colourful with smoothness. Diffuse reflectance thermal IR spectra were measured with an A2 Technology Exoscan FTIR spectrometer (A2 Technology, 2010). Only the measurements in the LWIR (8–14 μm) were used. Like most diffuse reflectance spectrometers, a small spot on the surface was illuminated with a broad-band source, and the energy reflected was measured at some range of off-nadir angles.

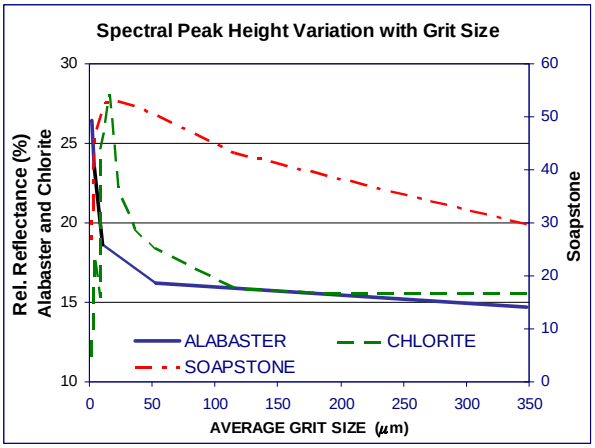

Figure 2. Plots of the spectral peak heights with mean grit size of the sandpaper used to roughen the rock. This is not the same as the actual roughness of the surface, but it is proportional to it.

The measurement is only truly diffuse reflectance if the surface is a diffuse reflector, and then Kirchhoff's Law holds: reflectance, ρ, is related to emissivity, ε, by $\rho = 1 - \varepsilon$ at any wavelength. The measure of roughness effects used here is the height of the reflectance peak.

Figure 2 shows the height variation of the spectral features with grit size for all three rock types. At values of sandpaper grits greater than about 25 μm, diffuse reflectance decreases with roughness, albeit slowly, for all three rock types. Below 25 μm, the curves are very steep. Soapstone and chlorite, which are closely related (both are steatites) increase to a peak around 25 μm, while the alabaster diffuse reflectance decreases in this range. At roughness sizes near the size of the wavelength, non-linear scattering processes occur and reflectance is no longer dominated by interactions between facets. This might be seen in these measurements between 2 μm and 25 μm, with a possible transition out to 50 μm. Of course, sandpaper grit sizes do not actually represent the actual surface roughness. The surfaces were scanned with a Nanovea PS-50 (Nanovea, 2010) optical microprofilometer at a nominal resolution of 10 μm in x, y, and z. The sizes of the finest grits (1,000 US grit scale and higher) are below the resolution of the profilometer. Also, the measured root mean square RMS values of the rock surfaces are well below the average grit size of the sandpaper so the values of grit size cannot be interpreted as the same as the surface roughness, just proportional to it. The actual roughness for the very fine grits must be viewed with caution. Nevertheless, spectral peak heights do decrease with roughness down to spatial scales that approach the wavelength.

2.2 Gravel: Spectral Emissivity Retrieval

Highly accurate and precise measurements of spectral emissivity in the field are notably difficult to make for a variety of reasons, including characterization of "downwelling" radiance from the surroundings and sensor calibration and stability. In this work, careful measurements were made with an extremely well-calibrated and stabilized FTIR for different roughness, nadir angle, material type, and time of day. The retrieval of emissivity generally follows that described by Salvaggio & Miller (2001) and is conceptually simple. The

method as implemented in this work requires spectral radiance measurements of the target and a reference panel and the temperature and reflectance of the panel surface. The panel is assumed to be perfectly diffuse (or, more precisely, the directional properties of the panel and target are assumed to be the same), its reflectance is the same as measured in the laboratory, and atmospheric transmission between the target and the sensor is assumed to be neglectable. It also assumes that there is no temporal variation of atmospheric transmission.

The spectral radiance at the sensor can be written as

$$L_s(\lambda,T) = \varepsilon(\lambda)L_{BB}(\lambda,T) + (1-\varepsilon(\lambda))L^{\downarrow}(\lambda) \quad (1)$$

where L_s is the spectral radiance at the sensor, λ is wavelength, T is the material surface temperature, ε is the emissivity of the surface, L_{BB} is the blackbody spectral radiance at the surface (described by Planck's function) and $L^{\downarrow}$ is the downwelling radiance. Solving for $\varepsilon(\lambda)$ gives

$$\varepsilon(\lambda) = (L_s(\lambda,T) - L^{\downarrow}(\lambda)) / (L_{BB}(\lambda,T) - L^{\downarrow}(\lambda)). \quad (2)$$

$L^{\downarrow}(\lambda)$ is comprised of all the radiance on the surface from the surroundings. Surroundings include the atmosphere and any clouds, buildings, sensors, and people in the vicinity. Variable in space and time, downwelling radiance can be complex quantity, and it is often the largest error in this approach to emissivity retrieval. Assuming the panel is a diffuse reflector, we can estimate $L^{\downarrow}(\lambda)$ with

$$L^{\downarrow}(\lambda) = (L_p(\lambda) - \varepsilon_p L_{BB}(\lambda,T_p)) / (1-\varepsilon_p) \quad (3)$$

where the subscript p refers to the panel, T_p is invariant with wavelength and, for the panel and spectral range used, ε_p is constant with a value of 0.040 Neither T nor T_p could be measured well so they must be estimated from the data. For T, Planck's functions were draped on $L_s(\lambda,T)$ to define the T that best fit the spectrum, assuming the emissivity was 1.0 somewhere in the spectrum. To determine the temperature of the panel, we draped the Planck's function over the observed panel spectrum where the atmosphere is opaque.

Two gravel materials at three size classes were measured at three view angles, and on three different days. One gravel was a calcite with a sharp spectral feature and the other was a silicate with broad features. The three size classes had mean sizes of 0.8 cm, 1.5 cm, and 5 cm, and view nadir angles were 7°, 30 °, and 60°. Figure 3 shows that the expected patterns were not clearly observed for a 30° nadir angle. At any angle, the weakest features occurred for the largest size class, as expected, but the medium size class had the strongest features. This seems partly due to the sensor view to the south, with a large portion of gravel surfaces being shaded and cool and the small gravel could not maintain as large a temperature gradient across a smaller distance. The large gravel did have the biggest changes with view nadir angle. In any case, the expectation that spectral feature depths are inversely proportional to roughness seems to be an over-simplification: it can be modulated by other factors. It is useful to note that the repeatability of the retrievals was generally in the 1–2% range, with exceptions occurring when the downwelling radiance was large.

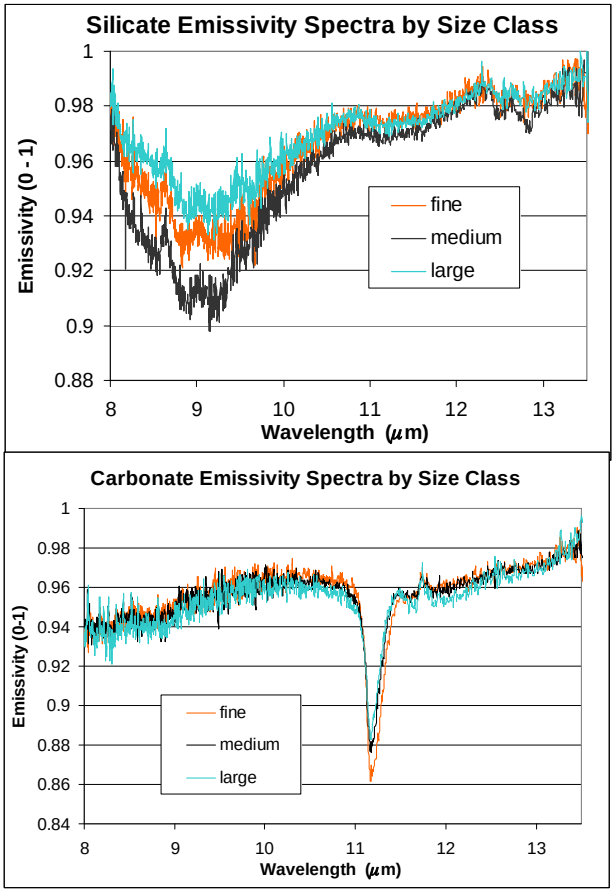

Figure 3. Retrieved emissivity spectra for gravels of different size classes for two rock types viewed at 30° from nadir.

2.3 Roughness Modelling and Validation

Radiosity models explicitly describe the radiant interactions between surface facets or points. Radiosity describes the radiative interactions between surface elements, and in the thermal IR domain includes both emitted and reflected energy. While these models can be scaled to any dimension, as a practical matter, areas of 1 m^2 are appropriate for high-resolution remote sensing simulations. Input digital elevation surfaces at 1 cm resolution can be easily measured with laser profilometers. Eq. 4 defines the radiosity for a number of facets or points:

$$B_i = R_i + \rho \cdot \sum_{j=1}^{n} B_j \cdot F_{ij}, \quad i,j = 1,2\ldots n \quad (4)$$

where B_i is the radiosity of a surface element i, R_i is thermal energy released from a surface element, ρ is reflectivity of the surface, F_{ij} is form factor from surface element j to surface element i, and n is the number of surface elements. The second term in equation (4) describes multiple scattering components—energy bounced one or more times among surface elements. The key step of the radiosity model is determining the form-factor matrix F. The basic form of a form factor is given by

$$F_{ji} = \frac{\cos\theta_i \cdot \cos\theta_j}{d^2 \cdot \pi} \cdot A_i, \quad (5)$$

where F_{ji} is the form factor from surface element j to surface element i, θ is the projection angle between the normal of a surface element and the line, linking the pair of elements together, A_i is the area of element i, and d is the distance between two elements (Figure 4).

The model simulates temperature and radiance variations due to roughness around some mean temperature over the course of a day. It is illumination and view angle-dependent, and while not explicitly spectral, it is wavelength-dependent and can be run for a series of spectra to simulate spectral changes. In this model, the mean temperature over time is determined by a simple heat diffusion model driven by environmental data. Mixed materials result in mixed spectra, and this can be simulated by assigning different properties to facets but assuming there is no difference of temperature..

Figure 5 shows a measured digital elevation model (DEM) of a rock surface in part a., shown graphically in part c. The DEM covers an area of 0.5 m by 0.85 m at sample spacing of 1 cm. Part b shows the change of simulated emissivity averaged over the area throughout the day. The roughness effect is largest when the sun is at moderate elevations. The DEM can then be multiplied by constants to rescale the roughness of the data. Part c shows the resulting calculation of broad-band emissivity over a range of RMS values.

The concept radiatively interacting surface elements can be extended to shapes and larger surfaces such as cracks, holes, and corners of surfaces. In these cases, terminology such as “cavity effects” and ”adjacency effects” are used. In fact, imaging spectrometer instruments show that even small cracks and holes become aspectral regardless of the spectra of the materials large when view factors exist.

Figure 6 shows observations and a simulation of the effects of two depressions (cavities) about 2 cm deep in a norite rock (plagioclase and hypersthene ± olivine). The norite has overlapping reststrahlen bands from 8.5 to 10.0 µm. Parts a and b show a photograph and a thermal IR spectral image of the rock. The thermal image was made with a Telops Inc, Hyper-Cam imaging FTIR spectrometer (Telops, 2010). Part c shows a micro-DEM of the rock smoothed to a 2 mm grid. Part d shows spectra taken from the image inside and outside the depressions. Finally, part e shows the simulated emissivity of the rock. In the depressions, the spectrum is shallower and higher than on the surface, becoming significantly more like a blackbody than the outer surface.

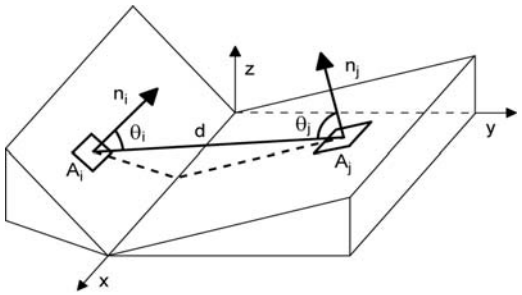

Figure 4. Schematic plot of the terms used in the form factor equation (Eq. 5).

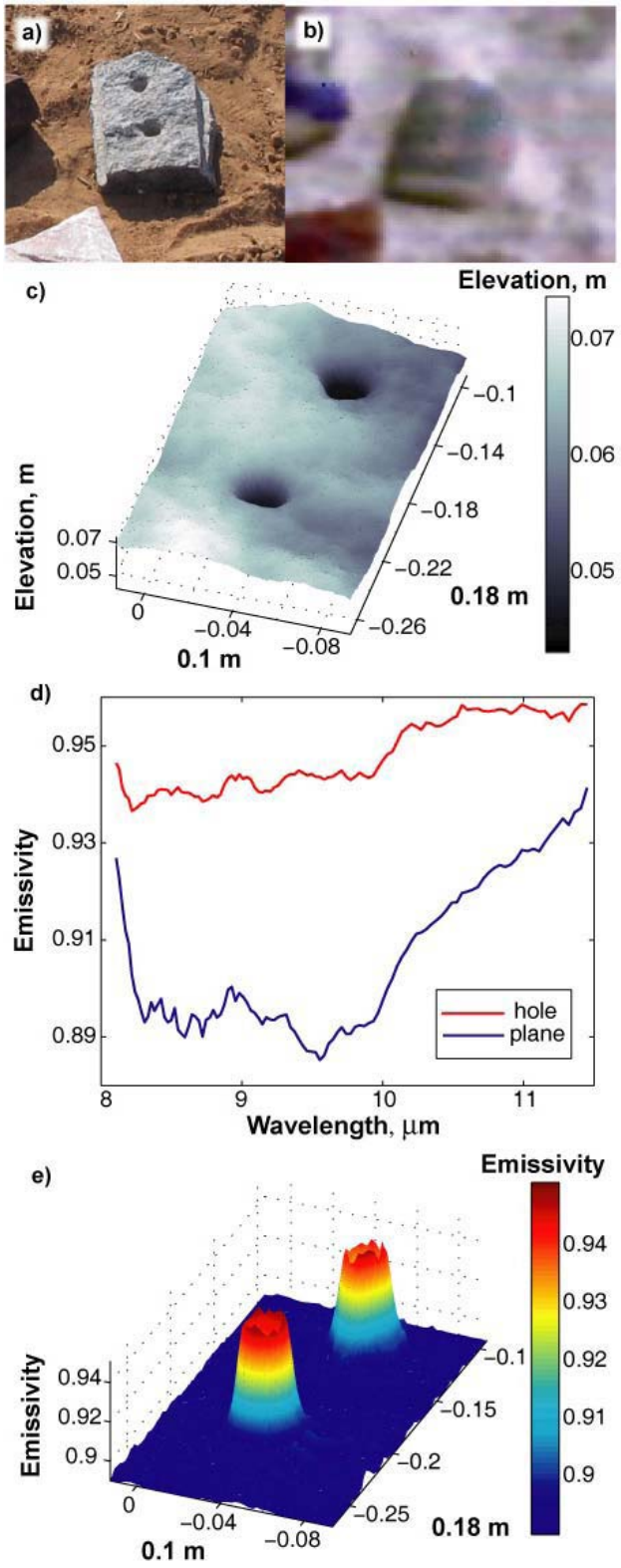

Figure 5. Simulated change of broad-band emissivity for a measured surface; the cavities in the rock become more like a blackbody than the outer surface; see text more explanation of the individual parts.

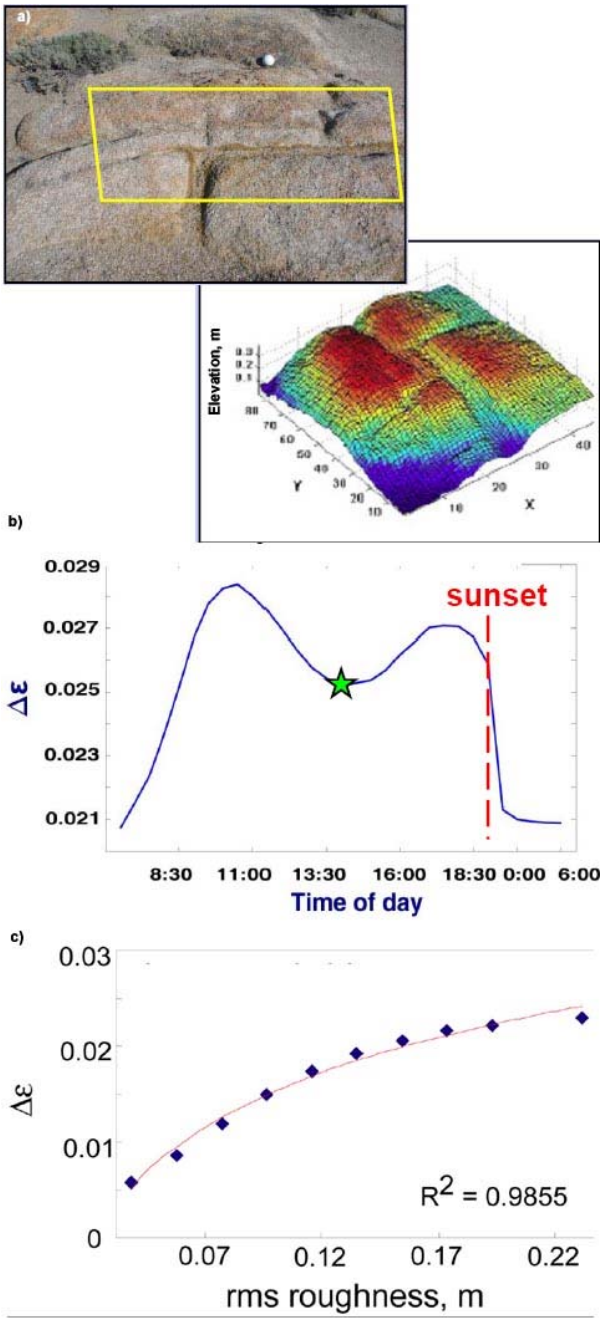

Figure 6. Simulated and observed effects of cavities on thermal IR spectra. See text for details.

Figure 7 shows another case where a form was created using plaster of Paris ($CaSO_4 \cdot 2H_2O \pm CaCO_3$) to facilitate model validation. The plaster has a single reststrahlen band centred near 8.6 µm. The form has two flat surfaces with different texture (roughness) shifted 7 cm and with a wall between them. The upper surface has hole that is 3 cm in diameter and 8 cm deep. In Figure 7, part a is a photograph of the Telops Inc. Hyper-Cam and the target; part b shows a hyperspectral image of the hole (and a crack that formed during transport); and part c is a Hyper-Cam image of the wall, and the upper and lower planes. Part d shows spectra taken from a Hyper-Cam image, and Part e shows the simulations at four spectral locations. The difference between the planes is the effect of roughness with the lower, rougher plane having a somewhat higher spectrum and a

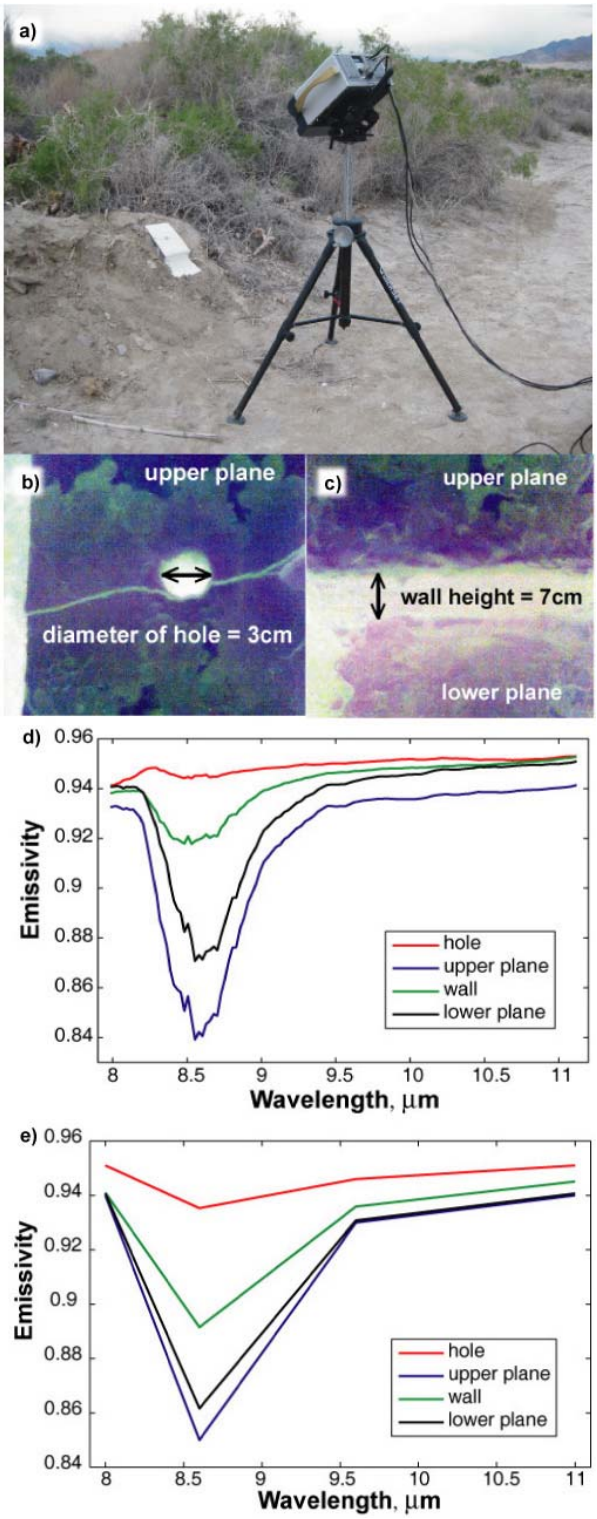

Figure 7. Simulated and observed spectra for a constructed plaster-of-Paris form. See text for details.

shallower spectral feature. The simulation did a good job on the spectral feature depth change, but not as good for the offset. The hole, both in the measurement and the simulation, had the highest emissivity spectrum, and very little of the spectral feature is present. The wall had a spectrum lower than the hole and with a clear but reduced spectral feature depth. The broad effects of radiosity were generally well simulated, impact of radiosity being proportional to view factors.

2.4 Roughness Retrieval from Directional Views

For practical applications, correcting for roughness effects on retrieved temperatures and emissivities requires remotely estimating surface roughness at sub-pixel scales. One approach that has been tested (Mushkin & Gillespie, 2005) uses bi-directional VNIR imaging, such as is available from ASTER, to estimate sub-pixel roughness at scales up to 15 m, the resolution of the acquired images. The approach makes use of differential sub-pixel shadowing in the 'down' and 'up' sun images as a relative proxy for roughness.. The relative measure of roughness is the DN ratio between the two images, corrected for path radiance using "dark-object subtraction"), with ratio values diverging from unity with increasing surface roughness. This ratio proxy roughness for roughness is largely insensitive to atmospheric effects, but must be calibrated to a quantitative measure of roughness, such as rms elevation. Calibration of the ratios to absolute values has been done from field measurement of micro-topography and modelling of shadows. The calibration is sensitive to regional topographic slope (within 5-10°), and sun elevation angle, and therefore requires re-calibration for each new application. A result of the calibration is shown in Figure 8. Older, smoother fans are darker (less shadowed); parts of the dry lake are smooth salt flats, and others are rough pinnacles of salt ~40 cm high.

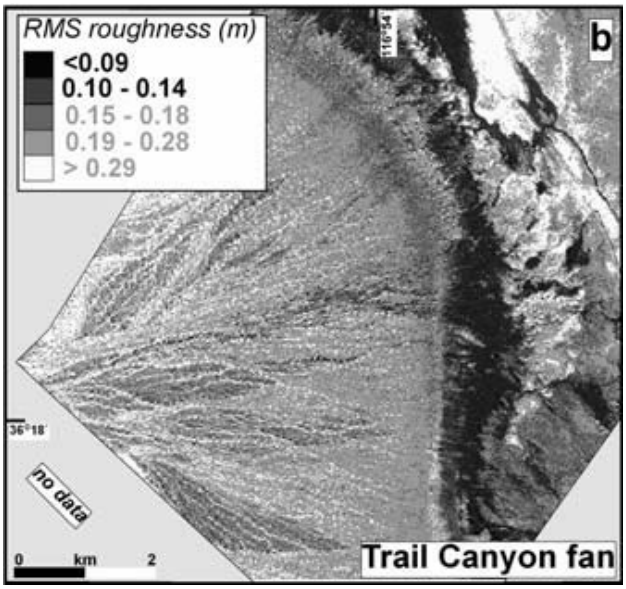

Figure 8. This is a sub-pixel roughness image calculated from two ASTER images of the Trail Canyon alluvial fan in Death Valley National Park. Image ratios were calibrated to roughness using field data.

3. SUMMARY AND CONCLUSION

Four studies look at the effects of surface roughness on the energy emitted by that surface. These studies cover spatial scales from sub-millimetre to tens of meters, and the effect of roughness across these scales is due to radiative interactions between surface elements. (There can also be a temperature effect, not discussed here.) The four studies represent different approaches to understanding the effects of surface roughness on thermal IR emittance. At sub-millimetre scales, roughness changes from sanding rocks alter diffuse reflectance by nearly a factor of two across the spectrum for the surfaces studied. Precise field measurements of radiance of gravel at centimetre scales did not clearly show expected trends of retrieved emissivity spectra as a function of roughness (size), and part of the reason seems to be the ability of individual gravel pieces to maintain a temperature gradient resulting from differential solar heating. Modelling and model validation measurements at the 1 to 10 cm scales show predictable changes of emissivity spectra with surface roughness: emissivity goes toward a black body for rough surfaces and in corners and shapes with a strong three dimensional form. The model is an abstraction, and its heat diffusion model is simplified. For many surfaces, this has not been a problem, but for surfaces with complex geometry (more than one value of z for an x, y location) or where three-dimensional heat diffusion is important, simulations of mean temperatures break down. Radiosity-produced variations can still be simulated. Although not discussed here in detail, compensation for roughness effects is possible given two or more images of the same area from different positions (with about the same resolution) and given knowledge of the roughness or valid simulations.

Multiple radiative interactions between surface elements do tend to drive observed spectra toward a blackbody spectrum even though the material properties are constant. The impacts are significant but variable and usually don't overwhelm the signal. The effects need to be quantitatively understood in order to understand thermal spectral measurements of most surfaces in the environment. However, surface roughness, while important, is one factor among many that modulate both the magnitude and spectra of ground-leaving thermal radiance and needs to be considered in context.

REFERENCES

Balick, L. K., M. E. Howard, H. M. Gledhill, A. Klawitter, and A. R. Gillespie, 2009. "Variation and sensitivity in spectral thermal IR emissivity measurements," IEEE WHISPERS, Grenoble, France. August 26-28, 2009.

A2-Technology, 2010, http://www.a2technologies.com/exoscan_handheld.html

Nanovea, 2010, http://www.nanovea.com/Profilometers.html

Mushkin, A. & Gillespie A. R. (2005). Estimating sub-pixel surface roughness using remotely sensed stereoscopic data. *Remote Sensing of Environment*, 99 (1-2), p.75-83

Salvaggio, C., and C. J. Miller, 2001, "Methodologies and protocols for the collection of midwave and longwave infrared emissivity spectra using a portable field spectrometer," SPIE, Image Exploitation and Target Recognition, Algorithms for Multispectral, Hyperspectral, and Ultraspectral Imagery VII, Volume 4381, April 2001.

Telops, 2010. http://www.telops.com/index.php?option=com_content&view=article&id=60&Itemid=59&lang=en

ACKNOWLEDGEMENT

This work was funded by the U. S. National Nuclear Security Administration, Office of Nonproliferation Technology Development and Treaty Verification, under contract DE-AC52-06NA25396 with Los Alamos National Security, LLC. LA-UR 10-01283